Supporting Information for

Energy Renormalization for Coarse-Graining the Dynamics of a Model Glass-Forming Liquid

Wenjie Xia*, Jake Song, Nitin K. Hansoge, Frederick R. Phelan Jr.,

Sinan Keten*, Jack F. Douglas*

*To whom correspondence should be addressed. Emails: wenjie.xia@nist.gov (W.X.), s-keten@northwestern.edu (S.K.), jack.douglas@nist.gov (J.F.D.)

Simulation information

All the molecular dynamics (MD) simulations including the all-atomistic (AA) and coarse-grained (CG) simulations are carried out using the Large-scale Atomic Massive Parallel Simulator (LAMMPS) package [1]. The AMBER force field [2] is applied to the AA simulations. The AA and CG simulations consist of 600 and 2 876 ortho-terphenyl (OTP) molecules, respectively, corresponding to 19200 atoms and 8628 CG beads. Periodic boundary conditions in all three dimensions are applied to the simulation box to model the bulk materials. An energy minimization using the conjugate gradient algorithm is performed for all the simulations [3], followed by two annealing cycles from 100 K to 700 K. Then, the systems are further equilibrated at 500 K for 4 ns. These simulations are performed using the NPT (i.e., constant number of particles, pressure and temperature) ensemble with fixed 1 bar pressure (i.e., 1×10^5 Pa). An integration time step Δt of 1 fs and 4 fs is applied to the AA and CG simulations, respectively. The dynamic properties (i.e., diffusivity, the Debye-Waller factor, mean-squared displacement and structural relaxation time) are calculated after equilibration run for 2 ns at each temperature.

Supporting Figures

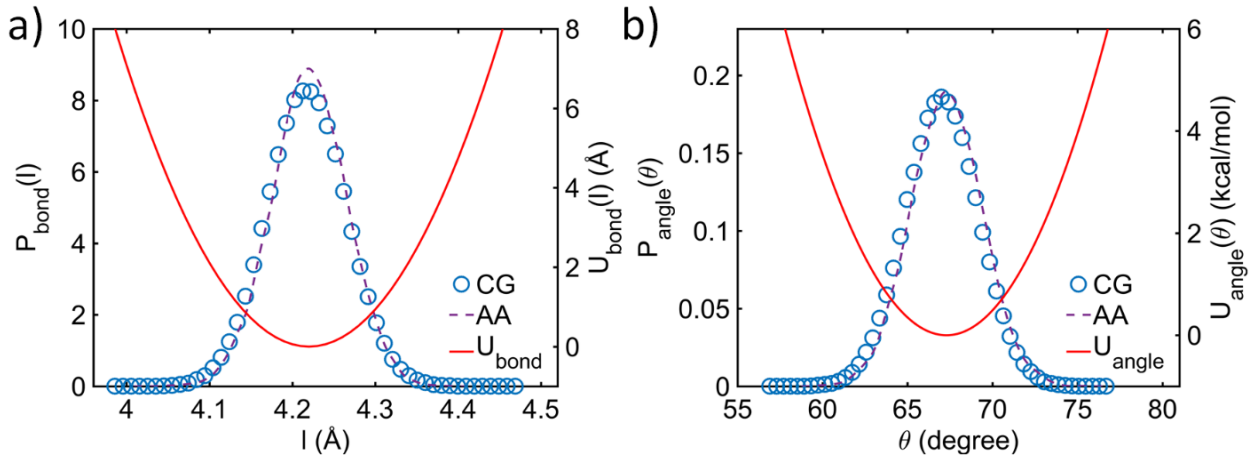

Figure S1. Probability distribution functions P of CG and AA models and the resulted CG potentials (i.e., U_{bond} and U_{angle}) derived from the inverse Boltzmann method (IBM) for the CG a) bonds and b) angles. The functional forms and parameters of U_{bond} and U_{angle} are summarized in Table S1.

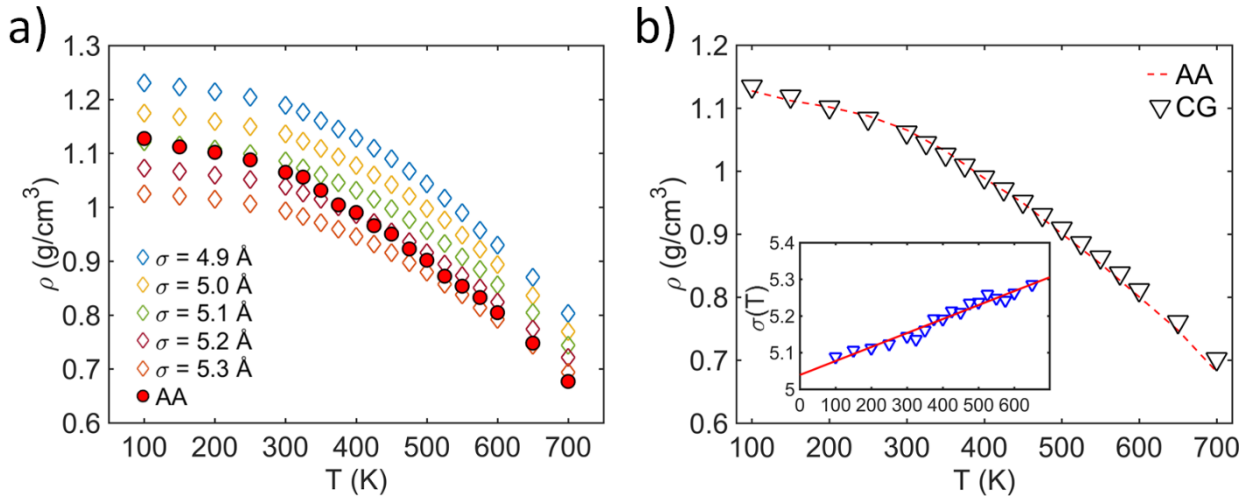

Figure S2. a) The density ρ vs. T for the AA and CG models with varying CG bead size through the LJ potential parameters σ. b) Comparison of the density ρ as a function of temperature T for the AA and CG models by introducing $\sigma(T)$. (Inset) The result of $\sigma(T)$ against T for the CG model by matching the T-dependent AA ρ. The line shows the linear fit to the $\sigma(T)$, which is listed in Table S2.

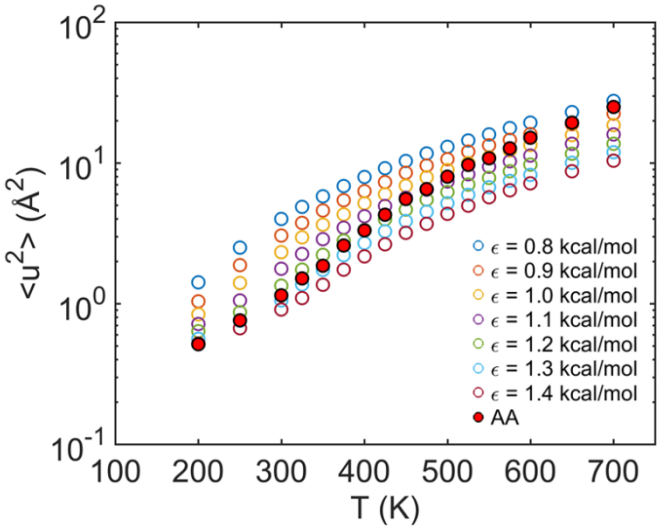

Figure S3. The Debye-Waller Factor $\langle u^2 \rangle$ vs. temperature T for the AA and CG models with varying cohesive interaction strength ε. The renormalization factor $\varepsilon(T)$ for the CG model is determined by matching T-dependent AA $\langle u^2 \rangle$, which is summarized in Table S2.

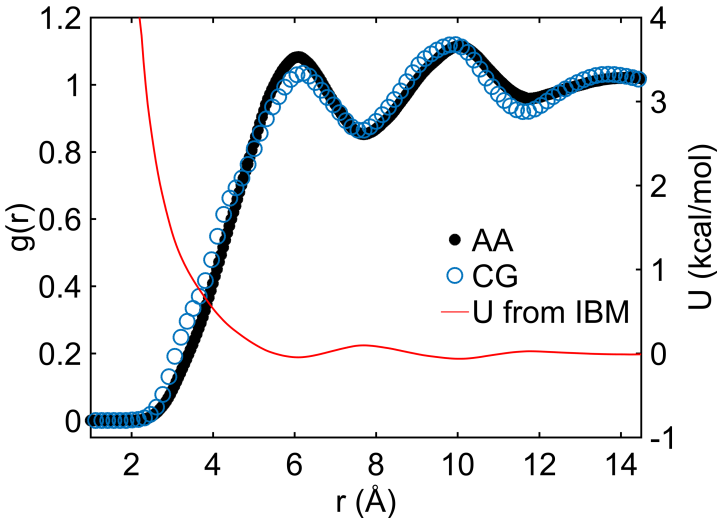

Figure S4. Comparison of the radial distribution function $g(r)$ of CG bead sites (i.e., the center of mass of each phenyl groups) for the AA and CG models using the IBM. The red line shows the CG nonbonded potential U derived from the IBM. The calculated diffusion coefficient D of the CG model from the IBM is much greater than the AA model and experimental values as shown in Figure 2 in the main manuscript.

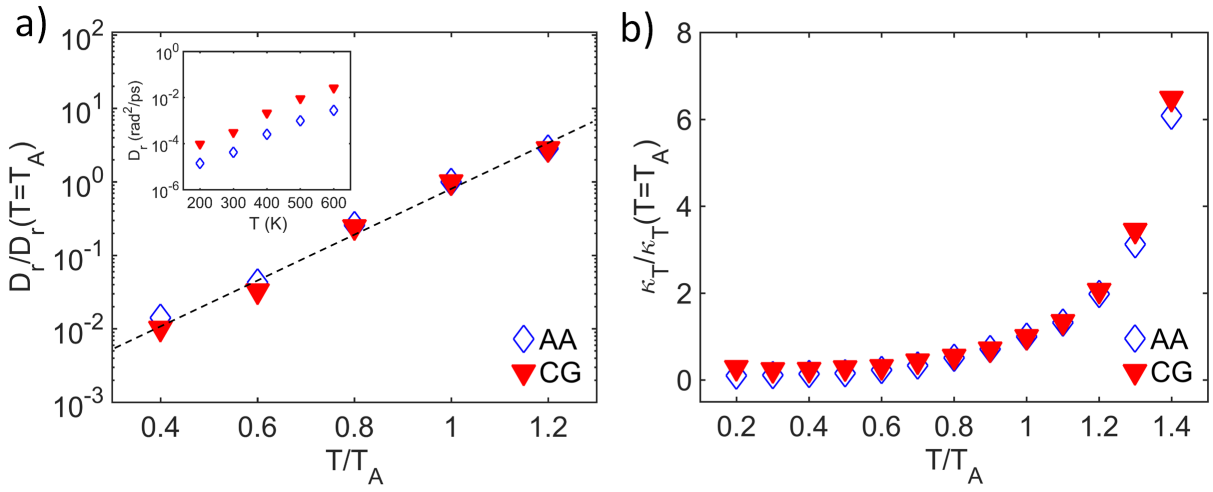

Figure S5. Energy renormalization prediction for the rotational diffusion coefficient D_r and isothermal compressibility κ_T (i.e., a basic fluid thermodynamic property) as a function of T. a) D_r normalized by its value at T_A for the AA and CG models as a function of T/T_A (i.e., $T_A \approx 500$ K for both AA and CG models). Linear line shows the data trend. (Inset) Comparison of the D_r vs. T for the AA model and CG model without normalization. b) κ_T normalized by its value at T_A as a function of T/T_A for the AA and CG models. These comparisons of D_r and κ_T in their normalized forms show a good consistency between the AA and CG models over a wide T range, which illustrate the necessity of making comparison to experiments and simulation models using appropriate reduced variables.

Supporting Tables

Table S1. Potential forms and parameters of the force field for the CG model of OTP.

Interaction	Potential form	Parameters
Bond	$U_{bond}(l) = k_b(l - l_0)^2$	k_b = 146.37 kcal/mol·Å^2 l_0 = 4.22 Å
Angle	$U_{angle}(\theta) = k_a(\theta - \theta_0)^2$	k_a = 218.40 kcal/rad^2 θ_0 = 67.29°
Nonbonded	$U(r) = 4\varepsilon(T)\left[\left(\frac{\sigma(T)}{r}\right)^{12} - \left(\frac{\sigma(T)}{r}\right)^{6}\right]$	$\varepsilon(T)$ and $\sigma(T)$, see Table S2

Table S2. Functional forms and parameters of the temperature-dependent nonbonded potentials of the CG model from the energy-renormalization method.

	Functional form	Parameters
$\varepsilon(T)$	$\varepsilon(T) = \frac{\varepsilon_A - \varepsilon_g}{1 + \exp[-k(T - T_T)]} + \varepsilon_g$	ε_A = 0.74 kcal/mol, ε_g = 1.41 kcal/mol $k = 0.0086$ K^{-1}, T_T = 475 K
$\sigma(T)$	$\sigma(T) = \sigma_a T + \sigma_0$	$\sigma_a = 3.8\times10^{-4}$ Å/K, σ_0 = 5.04 Å

Table S3. Summary of the characteristic temperatures predicted from the AA and CG models from the energy-renormalization method and their comparison with literature values. (The values are taken as the average over three samples with the standard deviation less than 4 K.)

Predictions	T_g (K)	T_0 (K)	T_A (K)	T_c (K)
AA	251	234	490	289
CG	249	231	490	291
Exp.	243 [4]	231 [4]	455 [5]	290 [6]

References

[1] S. Plimpton, Journal of Computational Physics **117**, 1 (1995).

[2] W. D. Cornell *et al.*, Journal of the American Chemical Society **118**, 2309 (1996).

[3] M. C. Payne, M. P. Teter, D. C. Allan, T. A. Arias, and J. D. Joannopoulos, Rev Mod Phys **64**, 1045 (1992).

[4] R. J. Greet and D. Turnbull, The Journal of Chemical Physics **46**, 1243 (1967).

[5] A. Tolle, Reports on Progress in Physics **64**, 1473 (2001).

[6] E. Bartsch, F. Fujara, M. Kiebel, H. Sillescu, and W. Petry, Berichte der Bunsengesellschaft für physikalische Chemie **93**, 1252 (1989).